Optimization of Process Parameters in Pulsed Current GTA Welding Process on ASTM 106 Grade-B Steel Pipes using Linear Regression

G Prakasham[1], L Siva Rama Krishna[2*], J Kandasamy[3]

[1,2] Department of Mechanical Engineering, University College of Engineering, Osmania University, Hyderabad – 500007,
[3]Maturi Venkata Subba Rao (MVSR) Engineering College, Hyderabad, Telangana, 501510
Email: sivaramakrisna.l@uceou.edu

ABSTRACT

The present research work aims to optimize the process parameters in the Pulsed Current Gas Tungsten Arc Welding (PCGTAW) process by employing the Design of Experiment (DOE) technique on ASTM 106 Grade-B Steel pipes. Taguchi method-based orthogonal array, L9 for four factors Pulse current (PC), Background Current (BC), Pulse Frequency (PF), and Pulse on time (PO) with three levels are employed. The higher the better reaction is picked to decide the ideal conditions for maximum ultimate tensile strength. The optimum values are found to be 220 A pulse current, 100 A background current, 4 Hz pulse frequency, and pulse on-time 50 %. ANOVA is implemented to gauge each factor's % contribution. The outcomes indicate that background current and pulse current are the significant process parameters to yield maximum ultimate tensile strength. Regression equations are used to model ultimate tensile strength, microhardness, and impact strength. Confirmation experiments are conducted to validate the results.

Keywords: *ASTM A106 Grade- B, Pulsed TIG welding, Taguchi, ANOVA*

1. INTRODUCTION

Many industrial applications need the use of welding, particularly when creating pipes. A specific welding method called pulsed current gas tungsten arc welding (PCGTAW) is used to join low-carbon steel products like ASTM A 106 Grade-B Steel pipes. Short, high-current pulses are used often during the welding process in PCGTAW, which enhances weld quality and minimizes thermal distortion. However, the PCGTAW process parameters, such as peak current, background current, pulse frequency, and pulse on time, have a significant impact on the quality. In this study, the ultimate tensile strength of ASTM 106 Grade-B Steel pipes produced by the PCGTAW method will be maximised by adjusting these process parameters. The Design of the Experiment (DOE) approach and the Taguchi method will be used to carry out the optimization. The study's findings will offer useful information for fabricating ASTM 106 Grade-B Steel pipes effectively and efficiently utilizing the PCGTAW method.

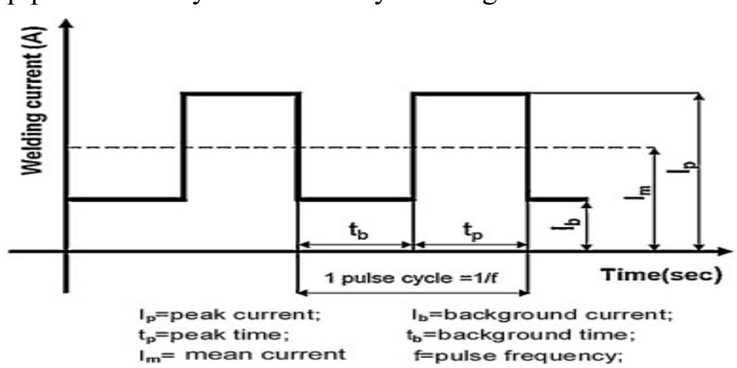

Figure 1: Pulsed TIG welding process

* Corresponding author: E-mail: sivaramakrisna.l@uceou.edu

2. Literature Review

Low carbon materials, like ASTM 106 Grade-B Steel pipes, are difficult to weld because of their great strength, toughness, resistance to corrosion, and ability to withstand high temperatures. Due to its enhanced weld quality and decreased thermal distortion, Pulsed Current GTA (PCGTAW) is one of the welding processes that has been widely employed for joining high-alloy materials. Due to its enhanced weld quality and decreased thermal distortion, Pulsed Current Gas Tungsten Arc Welding (PCGTAW) is one of the welding processes that has been widely employed for joining high-alloy materials.

Studies have revealed that the PCGTAW technique's process parameters have a considerable impact on weld quality. Peak current, background current, pulse frequency, and pulse on time are the most important variables. While a lower background current lowers the heat input and lessens thermal distortion, a higher peak current improves penetration and narrows the weld bead. While the pulse on time defines the length of the high-current pulse, the pulse frequency specifies how many pulses are applied every second.

Numerous researches have been conducted with the goal of enhancing the PCGTAW technique's process parameters to maximise ultimate tensile strength in high-alloy materials like ASTM 106 Grade-B Steel pipes. To determine the appropriate process parameters, this research made considerable use of the Taguchi method and the Design of Experiment (DOE) technique. Pulse Current Gas Tungsten Arc (PCGTA) welding achieves rapid solidification due to the decreased heat input, which is responsible for the fine microstructure. These pipes were linked utilizing a Tungsten Inert Gas (TIG) welding procedure with ER70S3 filler wire, with the root welded with 1.6 mm diameter wire and the finished weld with 2.5 mm filler wire. The combination of temperature cycles in the root and finish with low welding heat input results in a considerable change in the grains at the base metal as well as in the HAZ (Heat-Affected Zone). When extreme heat is utilized, the same results have not been documented [1]. Utilizing pulsed current GTA welding, ERNiCrMo-3 as a filler wire, and different junctions made of Monel 400 and AISI 316, the microstructure and mechanical characteristics of these joints are studied. Because of the thermal characteristics, the heat-affected zone is reduced and minor grain coarsening was found at the stainless steel's boundary [2]. Due to the low heat input provided to the base metal, the effects of filler metal on segregation and mechanical properties in AISI 904L material were improved, and migrated grain boundaries are visible at the weld zone of AISI 904L weldments [3]. Investigated the outcome of pulsed GTA welding on mechanical properties and microstructure, because the variation in the base and pulse current may reason for undercooling of the metal in the weld zone since heat input at weld pool is rapidly reduced in between pulse and background current of pulse tungsten inert gas welding [4 Pulse current results in a somewhat improved and more equiaxed grain structure in GTA welds. Surprisingly, typical persistent current welding produced predominantly columnar grain shapes. [5]. When compared to the conventional TIG welding process, the GTA welded AA (aluminium alloy) joint produced by pulsed current welding has superior ultimate tensile qualities [6]. The researchers investigated process parameter optimization in the pulsed TIG welding process of aluminium alloys by adjusting different gas mixes and discovered that the production of tiny dendritic microstructures resulted in the advancement of mechanical characteristics [7]. The metallographic examination reveals a fine grain structure at the weld pool, resulting in good mechanical characteristics. The current study is dedicated on obtaining the best process parameters in the PCGTAW process in order to achieve higher ultimate tensile strength.

3. EXPERIMENTAL PROCEDURE

ASTM 106 Grade- B steel pipe with 5 mm thickness and 50 mm outer diameter is shown in Figure 2. is carefully chosen for the present work the most common angles for V grooves are 600 (2×300). The land has generally required a width of 1mm and the root opening between the parts to be welded is 1.5 mm

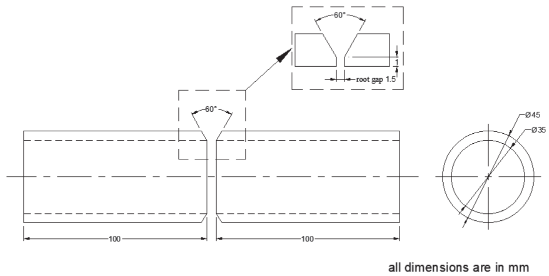

Figure 2: Schematic Diagram of ASTM 106 Grade B steel pipe

The chemical composition and mechanical properties of ASTM 106 Grade B steel are presented in Table 1 and 2.

Table 1: ASTM A 106 Grade B steel chemical composition

Element	Si	Ni	Mn	C	S	Mo	P	Cr	V	Cu
Weight (%)	0.27	0.014	0.60	0.21	0.01	0.007	0.015	0.057	0.001	0.017

Table 2: Mechanical Properties of ASTM A 106 Grade B steel

Hardness (Hv)	Tensile strength (MPa)	% Elongation	Yield strength (MPa)	Impact Strength (J)
160	410	32.2	303	128

Table 3: ER70S2 filler wire composition

Al	C	Cu	Mn	P	Si	S	Ti	Zr
0.10	0.06	0.15	1.10	0.012	0.50	0.012	0.10	0.09

Table 4: ER70S2 of filler wire mechanical properties

Yield Strength (MPa)	% Elongation	Ultimate tensile strength (MPa)
440	28	529

The PCGTAW experiments are conducted manually using the Indus Arc welding equipment and samples are shown in Figure 3. Taguchi design parameters and their levels are displayed in Table 3. The pipes are cleaned thoroughly before the conduction of experiments. Shielding gas of Argon with a flow rate of 14 lit /min. used to protect the weld pool with a constant speed of 2.09 mm/sec. to obtain maximum ultimate tensile strength.

Figure 3: Samples of ASTM 106 Grade B Steel pipes, weldments

The multiple linear regression method was employed as the primary method in this investigation. MINITAB is used to create the regression equations. Equation 1 shows the general form of multiple linear regression models.

$$y = \beta_0 + \beta_1 X_1 + \beta_2 X_2 + \beta_3 X_3 + \ldots\ \beta_n X_n \quad (1)$$

y = dependent variable

X_1, X_2, X_3 are independent variables

4. Results and Discussion

Table 5. lists the process variables and their ranges which were used in this study. Where X1, X2, X3, and X4 denote the pulse current, background current, pulse frequency, and pulse on, as well as their minimum and maximum values. The ASTM 106 Grade B steel pipes are joined using these range values.

Table 5: Factors and levels

Level	PC (A)	BC (A)	PF (Hz)	PO (%)
Notations	X_1	X_2	X_3	X_4
Range	180-220	100-120	4-8	40-60
Level 1	180	100	4	40
Level 2	200	110	6	50
Level 3	220	120	8	60

Table. 6 illustrates the results for ultimate tensile strength, impact strength, and microhardness derived from the experimental test conducted on 9 specimens utilizing the L9 orthogonal array while adjusting different process parameters. Process parameters are independent variables, while the produced values are dependent variables. The data in Tables 3 and 4 are modelled using the MINITAB software's linear regression.

$$y = \beta_0 + \beta_1 X_1 + \beta_2 X_2 + \beta_3 X_3 + \beta_4 X_4 \quad (2)$$

Table 6 shows the details of pulsed current GTAW experiments with different input process parameter levels to investigate the effect of input process parameters on output parameters. The Taguchi technique was used to adjust three of the four factors three levels, and all parameters were identified using an orthogonal array of L_9 (3^4) as the basis.

The arc efficiency for the pulsed current GTAW technique was set at 60%. The voltage was found to be 18V during the experiment. For the welding parameters PC, BC, PF, and Pulse on, a constant optimum welding speed of 2.09mm/sec was employed.

Table 6: Values of ultimate tensile strength, impact strength and microhardness

S. No	Control Factors				Ultimate tensile strength	Impact strength	Micro hardness
	PC	BC	PF	PO			
Units	A	A	Hz	%	MPa	J	Hv
1	180	100	4	40	464.66	100	201
2	180	110	6	50	458.06	102	202
3	180	120	8	60	460.29	114	204
4	200	100	6	60	467.80	113	200
5	200	110	8	40	460.45	101	197
6	200	120	4	50	456.01	105	207
7	220	100	8	50	470.05	111	189
8	220	110	6	60	468.28	118	199
9	220	120	4	40	455.31	102	203

The independent variables pulse current, pulse frequency, background current, and pulse on are represented X_1, X_2, X_3, and X_4 respectively. The recorded results become the dependent variables. The following fitted model was obtained as shown in equation 3 by using MINITAB.

Regression Equation for ultimate tensile strength

Where X_1, X_2, X_3 and X_4 represent the pulse current (PC), background current (BC), pulse frequency (PF) and pulse on (PO) respectively, while 'y' represents the ultimate tensile strength.

The fitted model is $y = 463.15 + 1.77 X_1 - 5.15 X_2 + 0.31 X_3 + 2.66 X_4$ (3)

The following confirmatory experiments were conducted and given in Table. 7 to verify the regression equation produced and the optimal values of affecting parameters. Contribution percentages for each parameter: pulse current (200A), base current (100A), frequency (4Hz), and pulse on (50 %). Other confirmatory trials selected from 3^4 arrays confirm the regression equation predicted for ultimate tensile strength fairly closely (Table 7).

Table 7: Confirmatory experiments

S.No	Control factors				Responses			
	Pulse current (A)	Back ground current (A)	Pulse frequency (Hz)	Pulse on (%)	Ultimate tensile strength, MPa (Average), (X)	Predicted Ultimate tensile strength, MPa (Y)	Differe nce (X-Y)	Error (%)
1	180	100	4	40	465.885	462.74	-3.14	0.006
2	180	110	6	50	458.145	460.56	2.42	0.005
3	180	120	8	60	458.755	458.38	-0.37	0.000
4	200	100	6	60	466.095	470.14	4.05	0.0086
5	200	110	8	40	456.89	459.98	3.09	0.006
6	200	120	4	50	459.27	456.87	-2.4	0.005
7	220	100	8	50	463.96	469.56	5.6	0.011
8	220	110	6	60	462.755	466.45	3.7	0.007
9	220	120	4	40	456.795	456.29	-0.41	0.000

Regression Equation for impact strength

The fitted model is $y= 88.33 + 2.50 X_1 - 0.50 X_2 + 0.50 X_3 + 7.00 X_4$ (4)
The following confirmatory experiments were conducted and given in Table 8 to verify the regression equation produced and the optimal values of affecting parameters. Contribution percentages for each parameter: pulse current (200A), base current (100A), frequency (4Hz), and pulse on (50 %). Other confirmatory trials selected from 3^4 arrays confirm the regression equation predicted for impact strength fairly closely (Table 8).

Table 8: Confirmatory experiments

S.No	Control factors				Responses			
	Pulse current, A	Back-ground current, A	Pulse frequency, Hz	Pulse on, %	Impact Strength (Average), MPa, (X)	Predicted impact strength, MPa, (Y)	Difference (X-Y)	Error (%)
1	180	100	4	40	100.32	97.83	-2.48	0.025
2	180	110	6	50	102.64	104.83	2.19	0.020
3	180	120	8	60	114.37	111.83	-2.54	0.022
4	200	100	6	60	113.89	114.83	0.94	0.008
5	200	110	8	40	101.91	100.83	-1.08	0.010
6	200	120	4	50	105.12	106.33	1.21	0.011
7	220	100	8	50	111.27	110.83	-0.44	0.0039
8	220	110	6	60	118.76	116.33	-2.4	0.020
9	220	120	4	40	102.02	102.33	0.31	0.003

Regression Equation for microhardness

The fitted model is $y= 202.56 - 2.667 X_1 + 4.000 X_2 - 2.833 X_3 + 0.333 X_4$ (5)

To verify the regression equation developed and validate optimized values of influencing parameters, the following confirmatory experiments were carried out and reported in Table 9. The percentage of contribution of each parameter pulse current (200A), base current (100A), frequency (4Hz), pulse on (50%). The regression equation predicted for microhardness is very close to other confirmatory experiments chosen among 3^4 arrays (Table 9).

Table 9: Confirmatory experiments

S.No	Control factors				Responses			
	Pulse current, A	Background current, A	Pulse frequency Hz	Pulse on, %	Microhardness (Average), (X)	Predicted microhardn ess(Y)	Difference (X-Y)	Error (%)
1	180	100	4	40	201.10	201.39	0.29	0.001
2	180	110	6	50	202.21	202.89	0.68	0.003
3	180	120	8	60	204.98	204.39	-0.59	0.002
4	200	100	6	60	200.56	196.55	-4.01	0.020
5	200	110	8	40	197.89	197.0	-0.89	0.004
6	200	120	4	50	207.34	207.05	-0.31	0.001
7	220	100	8	50	189.11	190.72	1.61	0.008
8	220	110	6	60	199.23	200.72	1.49	0.007
9	220	120	4	40	203.54	201.22	-2.32	0.011

Table.10 displays the regression model coefficients generated from equations 3,4,5 by inserting process parameters from table 7, 8, 9.

Table 10: Regression model coefficients

Regression coefficients	Ultimate tensile strength (MPa)	Impact Strength (J)	Microhardness (Hv)
β_0	463.15	88.33	202.56
β_1	1.77	2.50	-2.667
β_2	-5.15	-0.50	4.00
β_3	0.31	0.50	-2.833
β_4	2.66	7.00	0.333

The regression equations for ultimate tensile strength, microhardness and impact strength are

Ultimate tensile strength = $463.15 + 1.77 X_1 - 5.15 X_2 + 0.31 X_3 + 2.66 X_4$

Impact strength = $88.33 + 2.50 X_1 - 0.50 X_2 + 0.50 X_3 + 7.00 X_4$

Microhardness = $202.56 - 2.667 X_1 + 4.000 X_2 - 2.833 X_3 + 0.333 X_4$

5. Conclusions

The improvement of ASTM 106 Grade B steel pipe joints created by pulsed TIG welding was investigated using the linear regression technique. The goal of the study is to establish a relationship between process variables and microhardness, impact strength, and the ultimate tensile strength of ASTM 106 Grade B steel pipe welds. As a result, experimental study was undertaken using the L9 orthogonal array, as well as linear regression analysis, to estimate and analyse ultimate tensile strength, impact strength, and microhardness in pulsed TIG welding. The experimental and anticipated results at 220 A, 100 A, 4 Hz, and 50% show that pulse current and background current affect ultimate tensile strength.

References

1. Cleiton Carvalho Silvaa , Joaquim Teixeira de Assisb , " Residual Stress, Microstructure and Hardness of Thin-Walled Low-Carbon Steel Pipes Welded Manually, *Materials Research*. Vol 19, 2016, pp. 1215-1225. ISSN 1516 1439
2. B. Yelamasetti, G. Rajyalakshmi, and K. S. Kumar, "Mechanical and Microstructural Studies of Optimized Taguchi Grey Relational Analysis Of PCGTAW Process Parameters For Joining Monel 400 And AISI 316," *UPB Scientific Bulletin, Series B,* Vol. 83, Iss. 3, 2021 pp. 252-264, ISSN 1454-2331
3. K. Devendranath Ramkumar, "Effects of filler metals on the segregation, mechanical properties and hot corrosion behaviour of pulsed current gas tungsten arc welded super-austenitic stainless steel," *Journal of Manufacturing. Process.*, vol. 24, Oct. 2016 pp. 46–61. ISSN 1526-6125
4. Chennaiah MB, Kumar, Effect of Pulsed TIG Welding Parameters on the Microstructure and Micro-Hardness of AA6061 Joints, journal of materials science engineering, Vol 4, 2015, pp 1-4, ISSN 2169-0022,
5. G. M. Reddy, A. A. Gokhale, and K. P. Rao, "Optimisation of pulse frequency in pulsed current gas tungsten arc welding of aluminium–lithium alloy sheets," *Material Science Technology*, vol. 14, no. 1, Jan. 1998 pp. 61–66. ISSN 0267-0836.

6. N. Karunakaran and V. Balasubramanian, “Effect of pulsed current on temperature distribution, weld bead profiles and characteristics of gas tungsten arc welded aluminium alloy joints,” *Transactions Nonferrous Metals Society China*, vol. 21, no. 2, Feb. 2011, pp. 278–286, ISSN 1003-6326.
7. P. Kumar, K. P. Kolhe, S. J. Morey, and C. K. Datta, “Process Parameters Optimization of an Aluminium Alloy with Pulsed Gas Tungsten Arc Welding (GTAW) Using Gas Mixtures,” *Materials Sciences and Applications* , Vol.2 No.4, April 2011 ,pp 251-257, ISSN 2527-1034.
8. M.Sabzi, S.H.Mousavi, Anijdan, A.R.Eivani N.Park H.R.Jafarian “The effect of pulse current changes in PCGTAW on microstructural evolution, drastic improvement in mechanical properties, and fracture mode of dissimilar welded joint of AISI 316L-AISI 310S stainless steels”, Materials Science and Engineering: A Volume 823, 2021, pp 141700, ISSN 0921-5093.
9. A. Prithiraj, I. O. Otunniyi, P. Osifo, and J. van der Merwe, “Corrosion behaviour of stainless and carbon steels exposed to sulphate – reducing bacteria from industrial heat exchangers,” *Engineering Failure Analysis*, Vol No. 104, Oct. 2019, pp. 977–986, ISSN 1350-6307
10. M. Sarvghad, D. Del Aguila, and G. Will, “Optimized corrosion performance of a carbon steel in dilute sulfuric acid through heat treatment,” *Applied Surface Science*, Vol. 491, Oct.2019, pp.460–468, ISSN 0169-4332
11. M. Daavari, S. A. S. Vanini, E. Fereiduni, and M. H. Rokni, “Mechanical and electrochemical behaviors of butt-weldedhigh-temperaturee steel pipes,” *Engineering Failure Analysis*, Vol. 62, Apr 2016, pp. 287–299, ISSN 1350-6307
12. C. C. Silva, A. B. de Souza Neto, F. D. A. da Silva, F. E. S. de Freitas Júnior, and J. P. Farias, “Welding of ASTM A106 Gr. B steel pipes for high-temperature service – part 1 – residual stress analysis,” *Welding International*, vol. 23, no. 4, Apr. 2009, pp. 270–281. ISSN 1754-2138
13. Manikandan, M, Arivazhagan, N, Arivarasu, M. Mageshkumar, K, Rajan, Deva N., Murugan, B. Arul, Prasanth, P, Sukumar, S, Vimalanathan, R, “Analysis of Metallurgical and Mechanical Properties of Continuous and Pulsed Current Gas Tungsten Arc Welded Alloy C-276 with Duplex Stainless Steel,” *Transactions of the Indian Institute of Metals,* vol. 70, no. 3, Apr. 2017, pp. 661–669. ISSN 0972-2815.
14. R. Prabhu and, T. Alwarsamy, “Study and Investigations on Process Parameters for Bead Geometry during Cladding by Pulsed MIG Welding Process”. *Bluff Body Edge Effect on Pressure-Hill and Zone of Influence,* Vol No 8, 2014, pp 722-729.
15. A. H. V. Pavan, K. S. N. Vikrant, G. Vimalan, and K. Singh, “Metallurgical analysis of SA-106 Gr. B pipe failure during hot bending,” *Case Studies in Engineering Failure Analysis*, vol. 1, 2013, pp. 120–130.
16. S. S. M. Tavares, J. M. Pardal, R. R. Pinheiro, J. P. Gonçalves, and C. Scandian, “Failure of ASTM A-106 Gr. B tubes by creep and erosive wear,” *Engineering Failure Analysis*, vol. 26, Dec. 2012, pp. 337–343.